On the effects of straight metallic jewellery on the specific absorption rates resulting from face illuminating radio communications devices at popular cellular frequencies

W G Whittow[†], C J Panagamuwa[†], R M Edwards[†] and J C Vardaxoglou[†]

[†] Electronic and Electrical Engineering Dept., Loughborough University, Leicestershire, UK
E-mail: w.g.whittow@lboro.ac.uk, c.j.panagamuwa@lboro.ac.uk, r.m.edwards@lboro.ac.uk, j.c.vardaxoglou@lboro.ac.uk

Abstract. This paper presents simulated and measured phantom results for the possible effects that head worn jewellery may have on the relative levels of energy absorbed in the human head with cellular enabled mobile communications devices. FDTD electromagnetic code used with simple and complex anatomical mathematical phantoms were used to consider the interactions of metallic jewellery, heads, and representative sources at 900 and 1800MHz. Illuminated metallic pins of different lengths were positioned in front of the face. Initially, a homogenous phantom was used to understand the relative enhancement mechanisms. This geometry allowed the results to be validated with the industry standard DASY4 robot SAR measurement system related to the CENELEC head. Jewellery pins were then added to an anatomically realistic head. The relative increase in the 1g and 10g SAR, due to a pin with length 0.4 λ near the eyebrows of a complex, anatomically realistic head was approximately 3 times at 1800MHz. Such pins increased the SAR averaged over a 1g or 10g mass by redistributing the energy absorbed inside the head and focusing this energy towards the area of the head nearest the centre of the pin. Although, the pins increased the SAR, the SAR standards were not breached and the jewellery produced lower values than those of previous studies when the source was positioned close to the ear.

1. Introduction

This paper investigates the effects of straight metallic jewellery on the specific absorption rate (SAR) in the human head. In later sections, particular consideration is given to the choice of models and the choice of sources. The results presented are representative of the types of interactions from skin piercings for example studs in all parts of the head but more commonly the nose, the eyebrow and the ear; metallic spectacles particularly those with long straight sections are germane, as are hairclips. To investigate these electromagnetic systems we have used a rigorous Finite-Difference Time-Domain (FDTD) model with a continuous wave dipole source positioned in front of the head so as to illuminate the face. This will replicate a personal data assistant mobile communications equipment device (PDAMCE) used in front of, but away from, the face. This paper concentrates on the relative effects of metallic jewellery compared to a complete absence of jewellery making it applicable to all exposure conditions, such as field test engineers or military personnel. The paper has been designed so that it is applicable to other research, and the SAR results can be scaled.

It may be helpful, at this stage, to present a brief review of existing, closely, related papers. Typically, mobile phone research has been conducted for mobile communications equipment (MCE) positioned near the ear (Tinniswood *et al.*, 1998; Gandhi *et al.*, 1996; Dimbylow and Mann, 1994; Wainwright, 2000). However, the head has also been irradiated from in front of the eye using realistic mobile phone models (Wainwright, 2000; Martens *et al.*, 1995; Dimbylow and Mann, 1994). The authors have also briefly touched on the effect of metallic jewellery on the SAR in the head (Whittow et al., 2006) and this paper details a fuller extension of that work. Metallic implants inside the head have been found to increase the SAR (Cooper and Hombach,

1996). Virtanen has found that metallic implants can double the 1g SAR inside both a homogeneous phantom (Virtanen *et al.*, 2005) and inside a heterogeneous anatomical model of a head (Virtanen et al., 2007). The same author has reviewed the area of passive implants (Virtanen et al., 2006). The radiation efficiency of a dipole can be changed by using a passive reflector or a directive element (Tay et al., 1998). The head has also been irradiated with dipoles positioned near metallic walls both with a geometric head, (Cooper and Hombach, 1998) and an anatomical head (Bernardi et al., 1996). Both papers showed that metallic walls can increase the power absorbed in the head. The FDTD method has been used to examine thin metallic spectacles on a heterogeneous phantom with a resolution of 5mm (Troulis et al., 2001). The excitation used was a monopole on a metallic box positioned at the side of the head. The paper showed that metallic spectacles may re-distribute energy produced by an MCE. A drop in the efficiency of the MCE antenna was associated with an increase in SAR.

Measurements using a phantom and metallic spectacles showed that spectacles can affect the level of radiation near the eyes by ± 20dB due to shielding, enhancement, and depolarization effects (Griffin, 1983). For MCE operating at 835MHz, held by the ear, the SAR measured in the eye closest to the phone was found to increase by almost 30% (Anderson and Joyner, 1995).
A monopole on a metallic box was positioned by the ear of a human head wearing spectacles at 1.5GHz using the FDTD method (Wang et al., 1998). The average SAR in the eye increased by up to 2.7 times. The electric field magnitudes were shown to be comparatively low in-between the frames but increased just above the frames. Wang postulated that this increased SAR in certain parts of the head was due to current on the spectacles. The FDTD method with scaled models of an adult head was used to consider the effects of metallic spectacles on adults and children with a mobile phone placed by the ear (Joo et al., 2006). In the same paper, Joo also considered passive implants near the ear. Metallic ear rings have previously been considered with a source near the ear (Virtanen et al., 2007; Whittow et al., 2007; Fayos-Fernandes et al., 2006). In conclusion, whilst research has been undertaken on many related topics, the subject matter of this paper is novel.

1.1 Structure of the paper

This paper is structured as follows: Section 2.1 contains a description of the dipole as a source in our experiments; Section 2.2 includes a discussion of our choice of simulation phantoms and the types and properties of our models in FDTD. Initially, we use a homogenous phantom to understand the mechanisms and to validate the code with measurements. This then allows us to extend our investigations of jewellery to a realistic head model; Section 3.1 includes the initial results for a homogenous head with jewellery represented by pins. Section 3.2 details how metallic pins are representative of metallic jewellery, how they are modelled in FDTD, and provides validation for the results in Section 3.1; Sections 3.3 and 3.4 show results from the same system but with an anatomically accurate phantom head with many tissue types at 1800 and 900MHz; Section 3.5 summarises the 10g SAR values and compares the peak, 1g and 10g SAR results with previous studies in the literature.

2. Description of the Simulation

The independent 3D FDTD code in this work has already been used and validated with published controls in (Whittow and Edwards, 2004; Whittow and Edwards, 2005; Whittow, 2004). The code has previously shown good agreement with commercial software (Whittow et al., 2007) and Section 3.2 provides further validation of the results in this paper, by using SEMCAD X (Schmid & Partner Engineering AG, 2005) and DASY4 measurements. We have used Perfectly Matched Layers (PML), with geometric grading (Berenger, 1994), absorbing boundary conditions to terminate our grid. Our PML is eight cells thick and is positioned at least twelve cells from the head. Increasing the distance from the head to the PML was found to have negligible effect (Whittow, 2004). The Yee cell size used throughout this paper is 2mm. The lowest number of cells per wavelength was always greater than ten, and reasonable results have been obtained with only four (Dimbylow and Gandhi, 1991). The time step was 3.336pS. The simulations were run

for at least ten cycles and until stability was achieved (at least 1660 time steps at 1800MHz and 3340 at 900MHz).

2.1 Dipole wave source irradiation

We now continue with a short discussion with regard to the choice of source. In order to maximize future applicability, our experiments have been designed to allow validation wherever possible. In general, closed form analysis is not available for such complex systems as phone body interactions and therefore simulation, measurement and published controls have been used. Papers in this area of research have tended to use sources that fall into two distinct groups: sources that have associated phone structures, for example a metal box and perhaps some form of modulation; and more generic sources such as plane waves, monopoles and dipoles. λ/2 dipole models at 900 and 1800MHz have been used as the excitation in this paper. We believe our choice is justified as the dipole is a commonly used source that keeps the exposure system simple, repeatable and allows comparison with previous research (Schonborn et al., 1998; Keshvari and Lang, 2005). Here, in both measurement and simulation we have used a dipole several centimetres away from the head and the jewellery. As a result, the choice of excitation is less critical than in simulations where the phone is positioned next to the head, as the head has less impact on the effect of currents on the antenna and casing. We have not included models of the hand which reduces computational complexity and runtime (Dimbylow and Mann, 1994). Since the dipole is well understood, a dipole source allows the differences in absorption to be attributed properly to the jewellery rather than the source and its associated realistic metal box. In the FDTD simulations, the dipole was modelled by setting the tangential E-field components to zero along the length of the dipole (Taflove, 1995). The dipole used here is horizontally orientated along the Y axis (see Figure 1) and fed at its centre with a sinusoidal continuous wave. The input power of the dipole is 1W and the dipole is lossless. Note that communication devices operate with a duty factor of 1/8 not continuous wave, and the results in this paper can be scaled by 1/8th to create a time averaged SAR value (Dimbylow and Mann, 1994) (Wainwright, 2000). 1W radiated power is commonly used as it allows the results to be easily scaled because the SAR results are already in units of W/kg per W (Dimbylow and Mann, 1994).

A study using twenty adult volunteers was undertaken to measure the typical distance between the eye and screen of a PDA device when a user was reading text. The worst case scenario with the PDA closest to the face was 100mm. We therefore decided that to place the source at this distance was usefully representative. Using the condition $kr \cong 1$ for or near field boundary in which k is the wave number and r is the distance between field point and source; we see that our jewellery lies in the Fresnel region for both of our chosen frequencies.

2.2 The head model

For this research we have used three types of head model. Phantom 1 was a 200mm cubic homogenous head with the properties of brain simulating tissue (σ=1.37S/m, εr=40.48, ρ=1000kg/m³).

Phantom 2 had the same dimensions and electrical properties but had a 2mm outer shell made of fibreglass (σ=0S/m, εr=3.5). The use of Phantom 2 allowed our simulation results to be compared with the measurements made with the flat section of the Twin Specific Anthropomorphic Mannequin (SAM) phantom defined in IEEE 1528-2003, CENELEC 50361 and IEC 62209. Note; it is well known that the homogeneous head overestimates the SAR compared to an heterogeneous model and that the homogenous head, therefore, provides a conservative value (Gandhi, 1995). As it is very difficult to make SAR measurements in a heterogeneous head, the homogenous head remains a useful tool to complement simulations.

Phantom 3 was an anatomically realistic head provided by Brooks Air Force (www.brooks.af.mil/). The 3D head, which is based on The Visible Human Project, is that of an adult male and has twenty-five tissue types. The tissue properties at 1800MHz are given in (Whittow and Edwards, 2005). The head data has a 2mm resolution.

The three geometries used in this paper are shown in Figure 1 and are as follows; a half-wave dipole 100mm in front of a 200mm homogeneous cube, a 70mm dipole 98mm in front of a

200mm cube including a 2mm fibreglass open backed shell and a half-wave dipole 100mm in front of the eyebrows of a realistically shaped head.

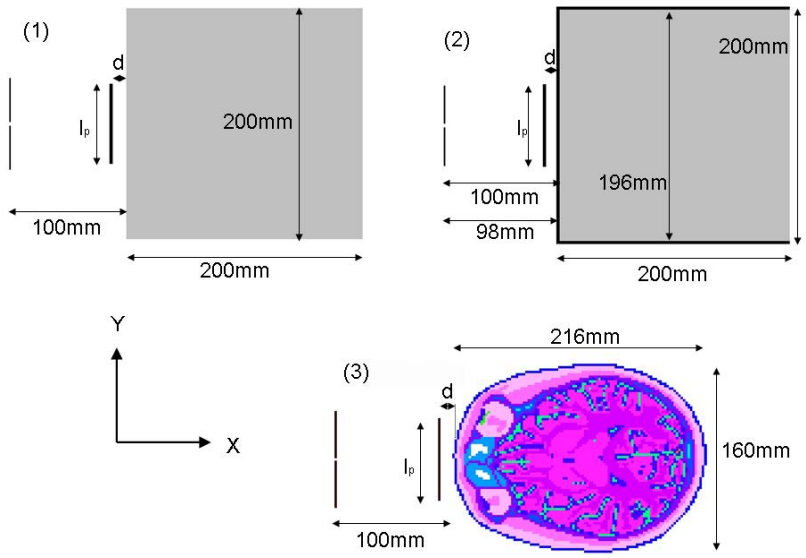

Figure 1. Orientation and geometry of dipole pin and head.

2.3. FDTD modelling of metallic pin jewellery

Typical jewellery that is easily modelled using representative pins includes most metal objects positioned close to the head, such as spectacle frames, the cross pieces of clip-on sunglasses used over plastic glasses, hairpins, corrective dental braces, various types of straight wire jewellery and skin piecing studs. There are an infinite number of shapes, sizes and positions of jewellery and as their effect is resonant (Whittow and Edwards, 2004), investigating specific shapes is less helpful than focusing on a range of general sizes and identifying the worse case scenario.

In FDTD, our metallic jewellery pins were modelled using Yee cells with the conductivity of copper (Whittow and Edwards, 2004). This technique has previously been used to model metal shapes (Nikita *et al.*, 2000; Bernardi *et al.*, 1996). Metallic spectacles have also been modelled by setting the conductivity of the Yee cells in the frames equal to titanium (Wang et al., 1998). Typical jewellery may be made of gold or silver and not copper. However, the authors (Whittow, 2004) have previously shown that the variation in conductivities of these metals is small and causes negligible variation to the SAR in the head. The jewellery pins investigated in this report were 2mm thick (1 Yee cell) and of different lengths; l_p, and different distances; d, from the phantom. The jewellery pins were orientated along the Y axis, parallel to the dipole, see Figure 1. For clarity, we will henceforth refer to jewellery pins as pins.

2.4 Specific absorption ratio and metrics

SAR is the standard criteria for measuring the amount of electromagnetic energy absorbed in the body and is calculated as in equation (1) where $|E|$ is the rms magnitude of the electric field strength vector, ρ is the mass density of the material in kg/m³ and σ is the electrical conductivity in S/m. The SAR is calculated with the twelve-field approach (Caputa et al., 1999).

$$SAR = \frac{\sigma |E|^2}{\rho} \qquad \text{(W/kg)} \qquad (1)$$

The metrics we have used in both measurement and simulation are the peak local SAR, the 1g SAR averaged over one gram of matter and the 10g SAR averaged over ten grams of matter. We have also included results of the total power absorbed in the phantoms.

Note that the maximum 1g SAR, defined by international ANSI/IEEE standards (used by the FCC in the USA) is 1.6W/kg (ANSI/IEEE, 1992). The 10g SAR is comparable to the European ICNIRP safety standards of 2.0W/kg (ICNIRP, 1998). Generally, the 10g SAR values in this paper behave in a very similar way to the 1g SAR values, except that the amplitudes are approximately half the 1g SAR values. For brevity and clarity, the 10g SAR results in this paper are listed in Section 3.5.

3. Results

3.1. Varying jewellery pin size and distance from Phantom 1 at 1800MHz

In this section, the source was a half-wave dipole at 1800MHz, orientated along the Y axis and positioned 100mm away from a homogeneous cubic head (Phantom 1), see Figure 1. Although, this simple phantom is not realistic, it is a useful tool to understand the relative enhancement mechanisms of pins near biological matter, as all parts of the pin are a constant distance from the phantom. The distance of the pin from the cubic phantom was varied along the X axis from 0mm (pin touching head) to 50mm from the phantom surface. At each position, the length of the pin was changed over the range 6 to 82mm. Figure 2 shows the results for the 520 simulations.

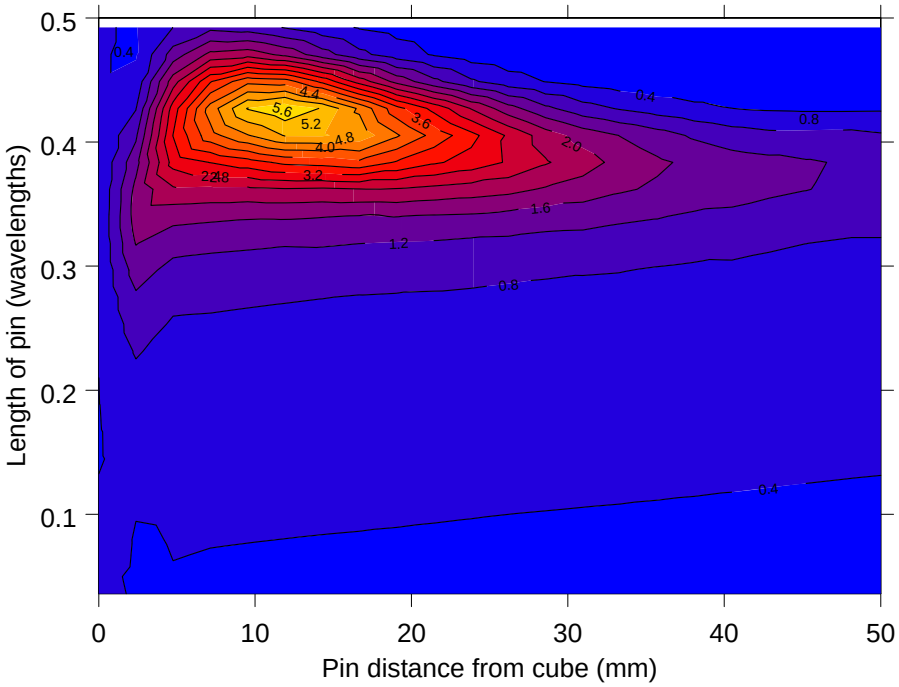

Figure 2. The 1g SAR (W/kg) in a cube as a function of the size of the pin and the distance from the pin to the cube.

Both the size of the pin and its distance from the phantom are important. The results in Figure 2 show that small pins <0.2 λ will have negligible effect on the 1g SAR regardless of the position. The effect becomes substantial when the length is greater than 0.3 λ. The maximum effect was seen with a pin 0.42 λ long. Longer lengths have a reduced effect on the 1g SAR. When the pin was either touching the head, or 2mm from the head, all jewellery sizes had little effect. The largest possible effect of the pin is when the distance from the cube to the pin is approximately 7 λ/100 (12mm). As the distance from the phantom surface is increased beyond

12mm the effect is decreased. Out of the 520 simulation permutations, 463 increased the 1g SAR. It was also found that the pin must always be longer than 0.24 λ to double the SAR.

The combination of a 0.42 λ pin at a distance of 12mm from the surface of the cube had the largest effect, increasing the 1g SAR by a factor of 16 (from 0.38W/kg without the pin to 6.12W/kg). These results are higher than the international safety standards of 1.6W/kg as the 1W power used is greater than standard mobile devices. The results are below the safety standards when they are scaled by 1/8th (the duty factor –see Section 2.1).The power absorbed in the whole cube with the pin was 0.18W, an increase of 30% (1.3 times) compared to without the pin.

Figure 4 to Figure 6 are related and should be viewed together. They show the SAR in the three planes illustrated in Figure 3; on the on the front surface of Phantom 1 in (a) and two cuts extending towards the back of the phantom in (b) and (c). Please see Phantom 1 in Figure 1 for the orientation and the geometry. Figure 4 shows the SAR without the pin. Figure 5 shows the SAR with the 0.42 λ pin. And Figure 6 shows the difference in the three SAR planes with the pin compared to without the pin (Figure 5 minus Figure 4).

Figure 4 shows that the location of the maximum SAR with no pin occurred at the centre of the front surface of Phantom 1. The addition of the pin caused a substantial increase in the SAR at this same location, see Figure 5. The shape of the maximum SAR with the pin mirrors the shape of the pin and is longer in the Y axis than in the Z axis. The pin also caused higher SAR values to extend deeper into the head, see Figure 5 (b) and (c). This could have implications for children who have smaller heads.

Comparison of Figure 4 and Figure 5 shows that there are also areas where the SAR is reduced when the pin is added. This can be clearly seen in Figure 6 which shows the difference in SAR due to the pin ($SAR_{pin} - SAR_{no\ pin}$). Figure 6 (a) demonstrates that the SAR is increased in a central elliptical area, near the pin, on the front surface of the cube (shown in red and black). However, the SAR, on the surface, outside this area was decreased with the pin (shown in blue and purple). The areas with the biggest decrease in SAR are parallel to, and either side of, the pin but shifted in the Z direction. The same pattern of increased SAR near the pin and decreased SAR away from the pin was seen as the distance into the cube increases along the X axis. The pin has negligible effect at the back of the cube as shown in Figure 6 (b) and (c).

These three diagrams clearly show that the resonant pin increased the SAR at the front of Phantom 1 in a cylindrical volume with an elliptical cross-section, and also that the pin decreased the SAR outside this volume. From this it can be deduced that the pin redistributes the electromagnetic waves absorbed over the entire surface of Phantom 1 and focuses them towards the area of the phantom that is closest to the pin, thus explaining how the total power absorbed increased by 1.3 times yet the 1g SAR increased by 16 times.

As a further validation, the PML region was moved 60 cells away from the source and dipole. Negligible differences were found in the 1g and 10g SAR. The power radiated into free space was calculated over a virtual surface by using the Poynting vector. Note this technique increases in accuracy as the distance from the source increases. The results are shown in Table 1. The pin increased the power in the head by decreasing the energy radiated in the Y and especially in the Z directions. Similar result were found for the difference in SAR in Figure 6 (a). The pin also increased the energy radiated away from the head in the –X direction.

Table 1. Power radiated into free space and absorbed in Phantom 1 (mW).

	–X direction	+X direction	Y direction	Z direction	Power abs in pin	Power abs in Phantom 1
No pin	210	4	128	535	-	136
Pin	320	3	104	393	0.3	178

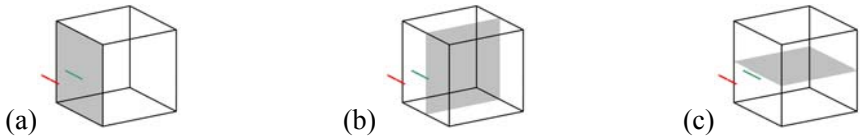

Figure 3. The three planar cuts which refer to Figure 4, Figure 5 and Figure 6.

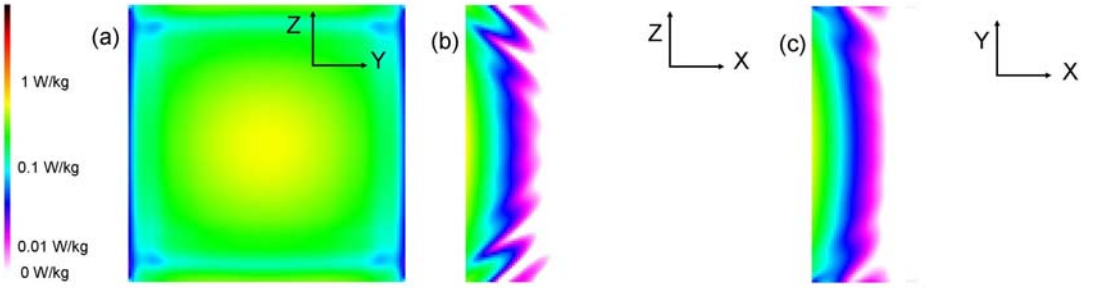

Figure 4. The SAR in Phantom 1 with no pin. (a) is on the front surface of the phantom. (b) and (c) are the two cuts to the back of the phantom through the centre of the cube.

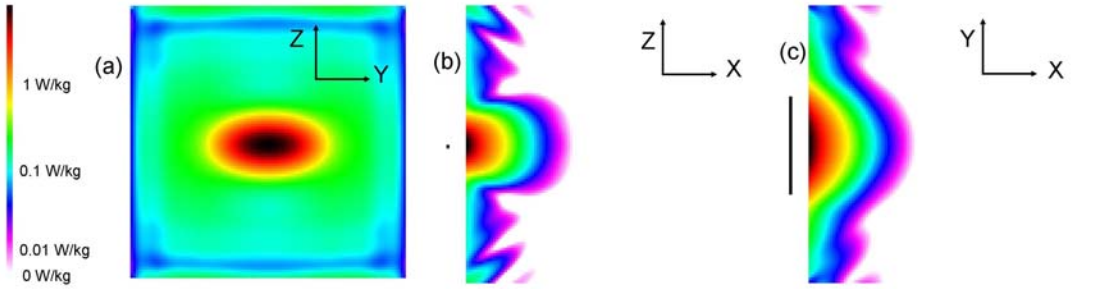

Figure 5. The SAR in Phantom 1 with 0.42λ pin. (a) is on the front surface of the phantom. (b) and (c) are the two cuts to the back of the phantom through the centre of the cube. NB The pin is included in (b) and (c).

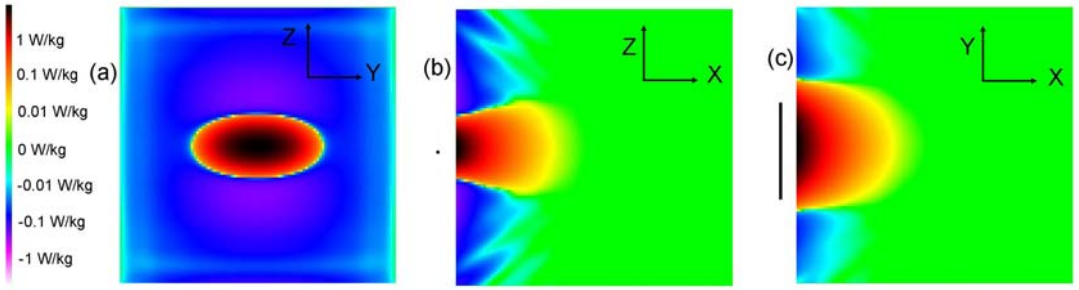

Figure 6. The difference in SAR with pin compared to without pin. (Figure 5 minus Figure 4); (a) is on the front surface of the phantom; (b) and (c) are the two cuts to the back of the phantom through the centre of the cube. NB The pin is included in (b) and (c).

It has been shown that a passive metal object of resonant size can increase and decrease the directivity of the dipole (Tay et al., 1998). Figure 2 shows that this resonant length is ~ 0.42 λ. This means that a greater proportion of the energy radiating from the dipole is directed towards the phantom with a certain size of pin. This effect can be investigated by using a plane wave source with a resonant pin 12mm from Phantom 1. When the polarization of the plane wave was in the same direction as the pin, the resonant pin increased the 1g and 10g SAR by 7.1 and 7.4 times respectively. The total power absorbed in the head increased by 19% (1.19 times). These results are less than with the dipole source and show that the resonant pin increased the directivity of the dipole towards the phantom. Clearly, however, there is an additional enhancement

mechanism as the pin increases the SAR, with the plane wave source. Fields incident on a resonant pin, induce a current on the pin. This current creates magnetic fields around the pin (Tay et al., 1998) and it is well understood that the SAR in the head is related to the square of the magnetic fields outside the phantom (Tay et al., 1998; Kuster and Balzano, 1992). The currents on the pin, have a focusing effect, and redistribute the energy in the phantom towards the area behind the centre of the pin, as shown in Figure 6. When the pin is moved further from the head, the coupling of electromagnetic energy between the pin and the head is small (Tay et al., 1998) and the magnetic fields close to the head are reduced. As the pin is moved closer to the head, the currents on the pin are out of phase with the surface currents on the phantom and cancel each other out (Tay et al., 1998). Therefore, the maximum SAR occurs when the pin in an optimum distance from the phantom, see Figure 2.

3.2. Validation of simulated effects of jewellery by measurements of SAR with DASY4 system and Phantom 2

Previously, the authors have found good agreement with FDTD simulations and DASY4 measurements with circular jewellery (Whittow et al., 2007). In order to validate the FDTD results in Section 3.1, we conducted two experiments using the flat section of the Twin SAM phantom of the DASY4 measurement system (Schmid et al., 1996). To allow for the features of the DASY4 our FDTD model was slightly altered (please see Phantom 2 in Figure 1).

A 70mm long pin was positioned 10mm away from the surface of the phantom and orientated parallel to the dipole. Results were normalized to 1W input power. The shell was 98mm from the centre of the dipole with the liquid being 100mm away from the dipole. The measurement set-up is shown in Figure 7. Note, the dipole in the measurements was 72.5mm long and had a diameter of 3.66mm. The pin was attached to the underneath of the flat phantom using cotton and clear sticky tape. Plumb lines and lasers were used to ensure that the alignment and position of both the pin and dipole were as accurate as possible.

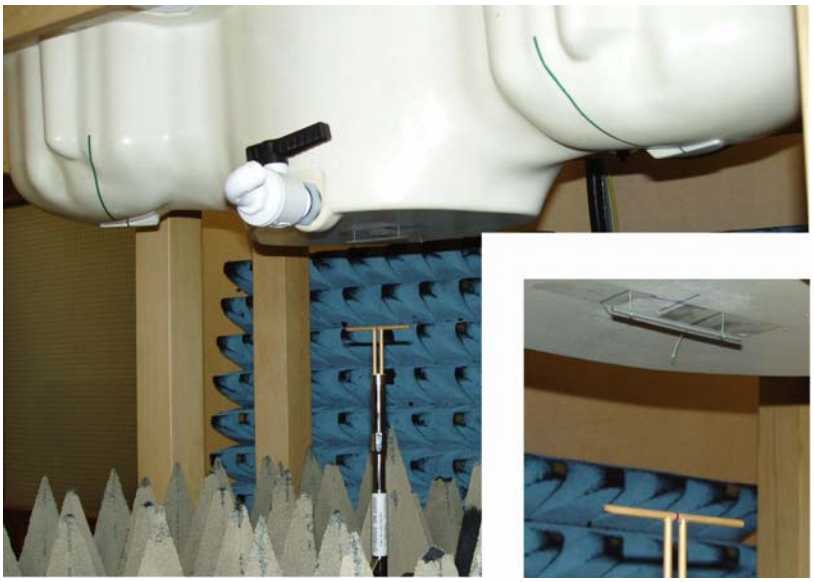

Figure 7. The measurement set-up with the DASY4 system. The 72.5mm dipole was positioned 98mm away from the flat section of the twin SAM phantom. A 70mm pin was hung 10mm below the phantom.

The 1g SAR results with the 70mm pin, 0 and 10mm from the flat fibreglass shell are shown in Table 2. The DASY4 results show good agreement with the FDTD code and the SEMCAD X (Schmid & Partner Engineering AG, 2005) simulations and show that the pin 10mm from the shell substantially increased the 1g SAR. The 70mm pin had little effect on the 1g SAR when it touched the fibreglass shell.

Table 2. The 1g SAR (W/kg) with and without the 70mm jewellery pin positioned 0 and 10mm from the flat fibreglass shell.

	Just head	Pin 0mm from shell	Pin 10mm from shell
DASY4 (Measured)	0.45	0.43	5.17
FDTD	0.40	0.42	5.24
SEMCAD X	0.37	0.37	5.28

Results are shown for the SAR along two different axes for the simulations and measurements in Figure 8 (Z axis, perpendicular to pin) and Figure 9 (Y axis, parallel to pin), with a 70mm pin 0 and 10mm from Phantom 2. Note, the SAR is calculated 1mm into the brain in the simulations and extrapolated to 1mm into the liquid with the DASY4 measurements. The simulation results show good agreement with the measurements. This clarifies that the reflections from the edges of the cube seen in Figure 4 (b) are not substantial, as the measurement phantom in Figure 7 is a different shape from Phantom 2.

Figure 8 shows that the local SAR on the surface is substantially increased near the pin, at the centre of the phantom, when the pin is 10mm from the shell. Local SAR values were increased to 8W/kg. When scaled by the duty factor, these values are lower than found by other authors with sources near the ear, (see Section 3.5). The 70mm pin, 10mm from the shell, increased the SAR in the approximate range; -22mm < Z < 22mm. Outside this range, both the simulations and the measurements showed that the presence of the pin decreased the SAR.

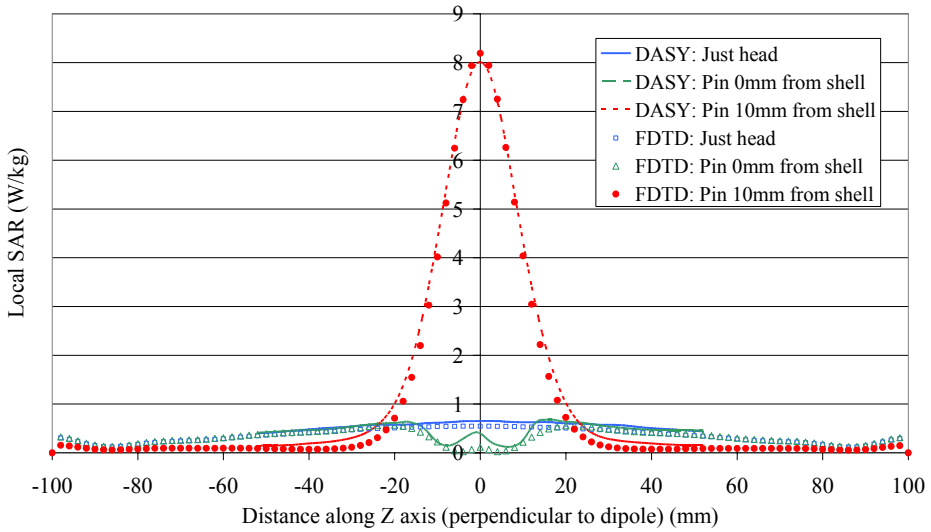

Figure 8. Comparison of FDTD simulations and DASY4 measurements of local SAR on the surface of Phantom 2, perpendicular to the dipole.

The local SAR parallel to the pin is shown in Figure 9. Again there is good agreement between the simulations and the measurements. The figure is similar to the SAR along the Z axis shown in Figure 8. With the pin 10mm from the shell, the SAR on the surface is increased near the pin, at the centre of the phantom, in the approximate range; -44 < Y < 44. Outside this range

the SAR was marginally decreased. Note that the two figures are similar except that the range where the pin increased the SAR is larger in the Y axis. The local SAR 1mm into the cube is increased near the centre of the pin and decreased outside this region. This region of increase is orientated parallel to the pin and has approximate dimensions of 88 × 44mm in the Y and Z axes. The measurement results in this section, therefore, reaffirm the ones in Figure 6 (a) that showed that the SAR is increased near the pin and decreased away from the pin. These measurements show that the pin has a focusing effect.

When the pin touched the shell, the pin had negligible effect on the 1g SAR values, see Table 1. However, the pin had a shielding effect and the location of the maximum was shifted 20 to 30mm away from the pin in the Y and Z directions as seen in Figure 8 and 9. Again, measurements showed good agreement with FDTD simulations with a pin touching the shell.

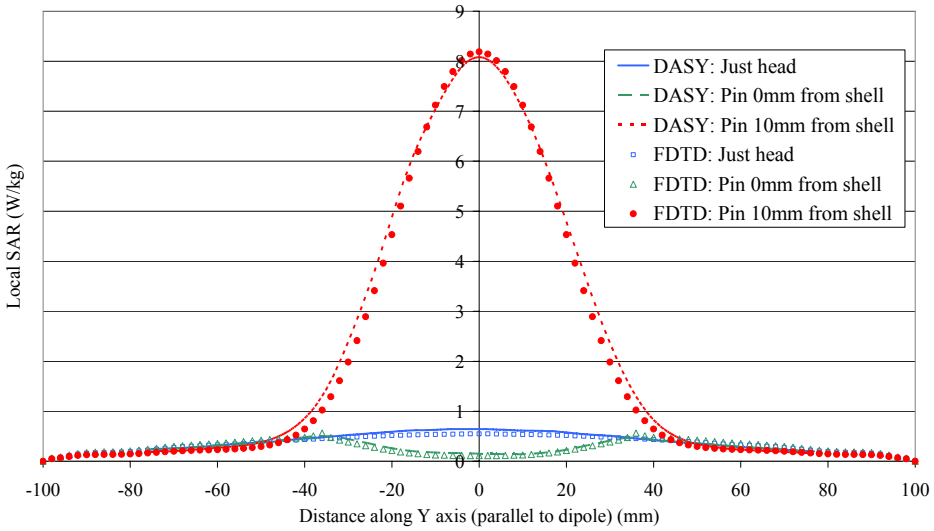

Figure 9. Comparison of FDTD simulations and DASY4 measurements of local SAR on the surface of Phantom 2, along an axis parallel to the dipole.

3.3 Simulated horizontally aligned jewellery near a heterogeneous head

In this section, a heterogeneous model with 25 tissue types is used; see Phantom 3 in Figure 1. The dipole and pin were positioned at the height of the eyebrows. The results are shown in Figure 10 and are similar to the ones with the pin and the cube shown in Figure 2. If the pin is 6 or 12mm away from the head; a 0.42 λ long pin has a substantial effect on the maximum 1g SAR and there is relatively little effect with much shorter or much longer pins. There is no secondary resonance when the pin is approximately 0.25 λ or 1 λ long. The largest SAR was found with the 70mm pin positioned 12mm from the head. This pin increased the power absorbed in the head from 0.11W to 0.14W (24%) and increased the 1g SAR by 2.5 times from 1.08 to 2.71W/kg. These values are smaller than the safety limits when scaled by the duty factor (1/8th).

The relative enhancement in 1g SAR due to the pin is smaller with the anatomically realistic head (×2.5) than with Phantom 1 (×16) and for the homogenous version of the same anatomically shaped head (×5.9) (Whittow et al., 2006). This difference was found to be caused mainly by the difference in exterior shape, but also by the differences in the internal tissue properties and was not due to the internal air in the sinuses behind the forehead (Whittow et al., 2006). Virtanen has also reported different relative enhancements of SAR when the tissues are changed (Virtanen et al., 2005). Section 2.2 mentioned that the homogeneous head provides a higher SAR value than the heterogeneous head. However, these results show that the homogeneous head also produces larger relative enhancements with metallic jewellery. Therefore, results with metallic jewellery using homogeneous phantoms are useful to validate simulations but may overestimate the expected SAR values in a human. It is possible, that different jewellery pins, at different

frequencies, in different locations relative to the body or on different human models may have larger relative effects than reported in this paper. Therefore, SAR measurements using a flat phantom with metallic objects in the vicinity may represent a very conservative worst case scenario. However, these results should raise concern about the validity of using the homogeneous head when developing guidelines in certain situations as the over exaggeration of SAR values may not be scientifically useful.

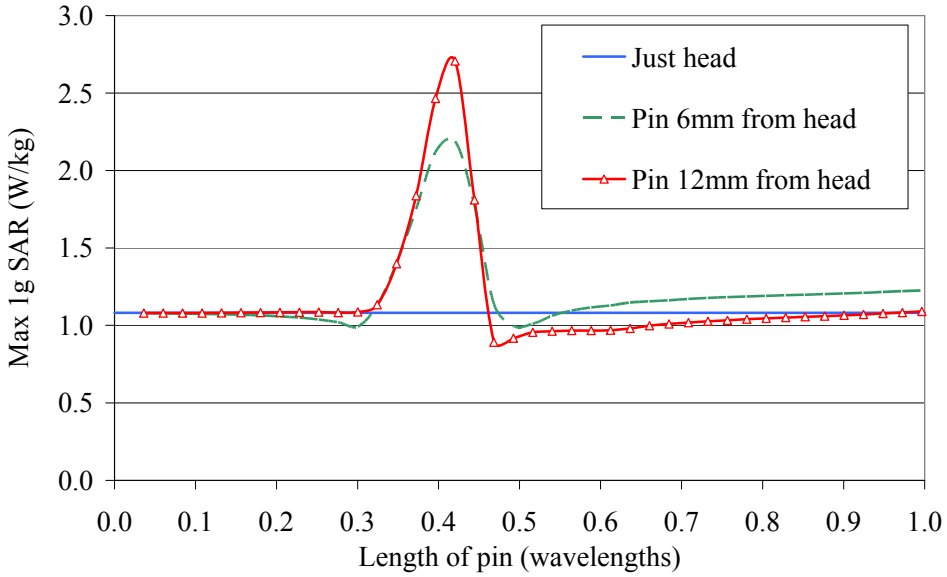

Figure 10. The heterogeneous Brooks head excited at 1800MHz. A horizontal metal pin has been added 6 and 12mm in front of the eyebrows.

3.4 Horizontal pin near a heterogeneous head at 900MHz

Metallic pins positioned 6, 12 and 20mm in front of the heterogeneous Brooks head were investigated with a half-wave dipole at 900MHz. The geometry used was the same as used in section 3.3, see Phantom 3 in Figure 1, except that the dipole was longer and the tissue properties changed, as they are frequency dependent. The results in Section 3.3 showed that a 70mm long pin can increase the SAR at 1800MHz; it is therefore hypothesized that a longer pin could have similar effects at 900MHz. The results in Figure 11 show that a 146mm (~0.44 λ) long metallic pin positioned in front of the eyebrows substantially increased the SAR.

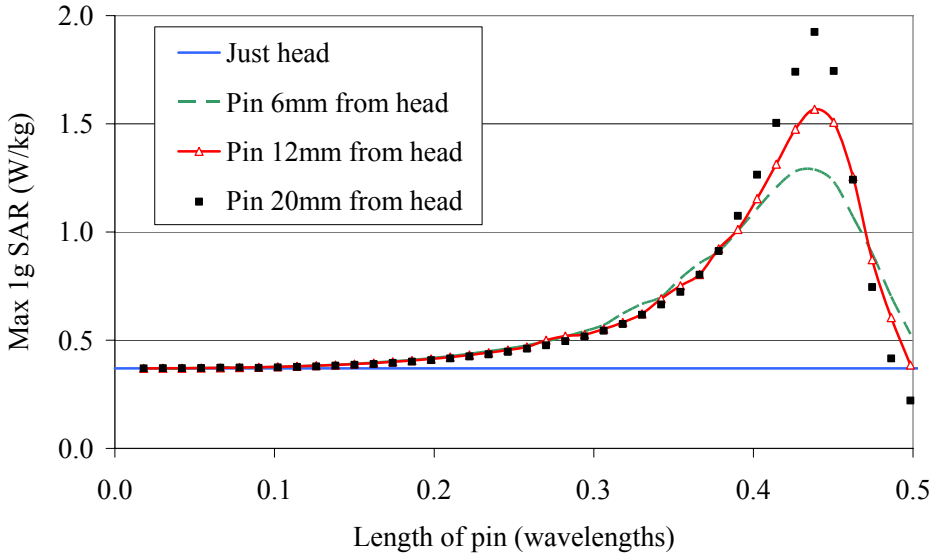

Figure 11. The heterogeneous Brooks head excited at 900MHz. A horizontal metal pin was added 6, 12 and 20mm in front of the eyebrows.

The maximum SAR in the head at 1800MHz occurred with the pin 12mm from the head. At 900MHz, a larger SAR occurs with the pin 20mm (6 λ/100) from the head than at 12mm (see Figure 11). The optimum size and distance of the pin can, therefore, be scaled with frequency. The power absorbed in the head was approximately doubled, with the resonant pin 20mm from the head, to 0.22W and the 1g SAR was increased by 5.2 times from 0.37 to 1.92W/kg. The results indicate that the relative enhancement of a resonant pin on the SAR in the Brooks head is greater at 900MHz than 1800MHz. Therefore, the size of the head in wavelengths affects the relative increase in the 1g SAR caused by the pin. It is interesting to note that the length of pin that resonates at 900MHz, 146mm (0.44 λ), has a close approximation to the width of a pair of metallic spectacles.

3.5 The effects of jewellery pins on the 10g SAR

Table 3 shows the 10g SAR results from the whole paper. The 10g SAR results with Phantom 2 show good agreement with DASY4 measurements and SEMCAD X commercial software. The 10g SAR in the anatomical head with a resonant pin increased by 3.5 times at 1800MHz and 5 times at 900MHz. The relative enhancement of the 10g SAR (×3.5) at 1800MHz is greater than the relative enhancement of the 1g SAR (×2.5). This is because the maximum 1g SAR location, without a pin, is at the bridge of the nose, while the 10g SAR is in the forehead and therefore directly behind where the pin was added. The 10g SAR values in the anatomical head do not break the SAR standards even before the duty factor is considered.

Table 3. The maximum 10g SAR values in Sections 3.1 to 3.4.

Section	Technique	Phantom	Frequency (MHz)	Pin length (mm)	Pin distance from head (mm)	10g SAR: Just head (W/kg)	10g SAR: With pin (W/kg)
3.1	FDTD	1	1800	70	12	0.25	3.25
3.2	DASY4	2	1800	70	10	0.29	2.79
3.2	FDTD	2	1800	70	10	0.27	2.74
3.2	SEMCAD	2	1800	70	10	0.25	2.86
3.3	FDTD	3	1800	70	12	0.45	1.59
3.4	FDTD	3	900	146	20	0.24	1.19

Table 4 compares the maximum peak, 1g and 10g SAR values with results from the literature. This paper has shown that metallic jewellery pins can substantially increase the SAR in the head. However, the values are less than other studies with a source positioned closer to the head. These results suggest that using a PDA with resonant metallic jewellery is likely to cause lower SAR values than using a mobile phone.

Table 4. Comparison with SAR results in the literature. All results are normalised to 1W.

Reference	Freq (MHz)	Geometry	Peak SAR (W/kg)	1g SAR (W/kg)	10g SAR (W/kg)
FDTD: With resonant pin	1800	Dipole 10cm from eye	7.7	2.71	1.59
(Van Leeuwen et al., 1999)	915	Dipole 2cm from ear	16.0	6.12	3.64
(Wainwright, 2000)	1800	Monopole by ear		8.06	3.74
(Dimbylow and Mann, 1994)	900	Dipole 2cm from eye		7.12	4.84
(Tinniswood et al., 1998)	835	Monopole by ear	18.9	3.98	

4. Conclusions and Discussion

This paper has investigated the effect of jewellery pins on the SAR in the head. Substantial relative increases in SAR have been found. However, the SAR values are always below the standard levels when the duty factor is applied. SAR levels in a PDA user, with metallic jewellery may be several times higher than without jewellery, but are smaller than values found with a mobile phone held by the ear. It is considered very unlikely that metallic jewellery could produce substantial heating effects in the head, but athermal effects cannot be ignored completely.

From the results with the cubic phantom, it can be inferred that the effects would be negligible with small straight jewellery touching the skin. The results indicate that metallic jewellery insulated from the head by air or a plastic coating may have a greater effect. At 1800MHz, straight jewellery, positioned approximately 12mm from the head, could have a substantial effect. Such objects could include metallic spectacles, microphones and nose and ear jewellery that may hang away from the head. Our results suggest that thin straight jewellery will maximize the effect on SAR when it is ~0.42 λ long. From observation, it was found that the majority of lengths and locations of simulated jewellery increased the 1g and 10g SAR but by less than a factor of two. The total power absorbed in the cubic head was found to increase by up to 1.3 times. In cubic phantom heads, the 1g SAR was found to increase by up to 16 times and the 10g SAR by approximately 13 times. These results were validated by measurements. The measurements and simulations showed that the SAR in an elliptical area at the front of the head near to the centre of the pin was increased as the pin focused the energy away from the edges of the head when viewed from the front. The pin also increased the directivity of the dipole.

Similar mechanisms were found with an anatomically realistic head. The relative effects of the jewellery on the 1g SAR was reduced from a sixteen fold increase for the homogenous cube to 2.5 times with the heterogeneous head. The cubic homogenous head is, therefore, a useful tool to understand the enhancement mechanisms and to corroborate simulations with measurements, but is likely to over-estimate the effect of the pin. At 900MHz, a 0.42 λ long pin was found to increase the 1g SAR by 5.2 times. Therefore, pins of similar size relative to a wavelength were found to cause similar resonances. At 900MHz, a 146mm pin caused the largest SAR; this is approximately the size of the crosspiece of a pair of semi-rimmed spectacles. At higher frequencies smaller metallic objects may be resonant.

Since available power, conductivity and permittivity are fixed, the above results point to there being increased levels of field strengths near the pin on the surface of the phantom as a result of the pin and head combination. One hypothesis is that fields from the source cause currents to flow in the head and that these currents cause fields in addition to those already generated by the source dipole. When a pin is brought close to the head, these additional fields cause current to flow on the pin which produces further fields. Depending on the distance of the

pin from the head, fields within the head are superimposed, constructively or destructively, leading to increases or decreases in SAR. It is therefore reasonable to view the jewellery and head as a resonant system with excitation from the dipole.

References

Anderson V and Joyner K H 1995 Specific absorption rate levels measured in a phantom head exposed to radiofrequency transmissions from analog hand-held mobile phones *Bioelectromagnetics* **16** 60-9

ANSI/IEEE 1992 IEEE standard for safety levels with respect to human exposure to radio frequency fields 3kHz to 300GHz *Standard C95.1-1992*

Berenger J P 1994 A perfectly matched layer for the absorption of electromagnetic waves *Journal of Computational Physics* **114** 185-200

Bernardi P, Cavagnaro M and Pisa S 1996 Evaluation of the SAR distribution in the human head for cellular phones used in a partially closed environment *IEEE Trans. Electromagn. Compat.* **38** 357-66

Caputa K, Okoniewski M and Stuchly M A 1999 An algorithm for computations of the power deposition in human tissue *IEEE Antennas Propag. Mag.* **41** 102-7

Cooper J and Hombach V 1996 Increase in specific absorption rate in humans from implantations *Electronic Letters* **32** 2217-9

Cooper J and Hombach V 1998 The specific absorption rate in a spherical head model from a dipole with metallic walls nearby *IEEE Trans. Electromagn. Compat.* **40** 377-82

Dimbylow P J and Gandhi O P 1991 Finite-difference time-domain calculations of SAR in a realistic heterogeneous model of the head for plane-wave exposure from 600MHz to 3GHz *Phys. Med. Biol.* **36** 1075-89

Dimbylow P J and Mann S M 1994 SAR calculations in an anatomically realistic model of the head for mobile communication transceivers at 900-MHz and 1.8-GHz *Phys. Med. Biol.* **39** 1537-53

Fayos-Fernandes J, Arranz-Faz C, Martinez-Gonzalez A and Sanchez-Hernandez D 2006 Effect of pierced metallic objects on SAR distributions at 900MHz *Bioelectromagnetics* **27** 337-53

Gandhi O 1995 Electromagnetic absorption in the human head from experimental 6-GHz handheld transceivers *IEEE Trans. Electromagnetic Compatibility* **37** 547-58

Gandhi O, Lazzi G and Furse C M 1996 Electromagnetic absorption in the human head and neck for mobile telephones at 835 and 1900MHz *IEEE Trans. Microwave Theory Technology* **44** 1884-97

Griffin D W 1983 A microwave antenna method of measuring the effect of metal-framed spectacles on microwaves near the eye. *Antennas and Propagation Society International Symposium* **21** 253-6

ICNIRP 1998 Guidelines for limiting exposure to time-varying electric, magnetic and electromagnetic fields (up to 300GHz) *Health Phys* **74** p. 494-522

Joo E, Szasz A and Szendro P 2006 Metal-framed spectacles and implants and specific absorption rate among adults and children using mobile phones at 900/1800/2100MHz *Electromagnetic Biology and Medicine* **25** 103-12

Keshvari J and Lang S 2005 Comparison of radio frequency energy absorption in ear and eye region of children and adults at 900, 1800 and 2450 MHz *Phys. Med. Biol.* **50** 4355-69

Kuster N and Balzano Q 1992 Energy absorption mechanism by biological bodies in near field of dipole antennas above 300MHz *IEEE Trans. Vehicular Technology* **41** 17-23

Martens L, Demoerloose J, Dezutter D, Depoorter J and Dewagter C 1995 Calculation of the electromagnetic-fields induced in the head of an operator of a cordless telephone *Radio Sci.* **30** 283-90

Nikita K S, Cavagnaro M, Bernardi P, Uzunoglu N K, Pisa S, Piuzzi E, Sahalos J N, Krikelas G I, Vaul J A, Excell P S, Cerri G, Chiarandini S, De Leo R and Russo P 2000 A study of uncertainties in modeling antenna performance and power absorption in the head of a cellular phone user *IEEE Trans. Microw. Theory Tech.* **48** 2676-85

Schmid & Partner Engineering AG 2005 SEMCAD-X Reference Manual.

Schmid T, Egger O and Kuster N 1996 Automated E-field scanning system for dosimetric assessments *IEEE Microwave Theory and Techniques* **44** 105 -13

Schonborn F, Burkhardt M and Kuster N 1998 Differences in energy absorption between heads of adults and children in the near fields of sources *Health Phys* **74** 160-8

Taflove A 1995 *Computational electrodynamics. The finite-difference time-domain method.* (Artech House, Inc.)

Tay R, Balzano Q and Kuster N 1998 Dipole configurations with strongly improved radiation efficiency for hand-held transceivers *IEEE Trans. Antennas and Propagation* **46** 798-806

Tinniswood A D, Furse C M and Gandhi O P 1998 Computations of SAR distributions for two anatomically based models of the human head using CAD files of commercial telephones and the parallelized FDTD code *IEEE Trans. Antennas Propag.* **46** 829-33

Troulis S E, Scanlon W G and Evans N E 2001 Effect of 'hands-free' leads and spectacles on SAR for a 1.8 GHz cellular handset. In: *1st Joint IEI / IEE Symposium on Telecommunications Systems Research,* (Dublin, Ireland) 1675-84

Van Leeuwen G M J, Lagendijk J J W, Van Leersum B J A, Zwamborn A P M, Hornsleth S N and Kotte A N T J 1999 Calculation of change in brain temperatures due to exposure to a mobile phone *Phys. Med. Biol.* **44** 2367-79

Virtanen H, Huttunen J, Toropainen A and Lappalainen R 2005 Interaction of mobile phones with superficial passive implants *Phys. Med. Biol.* **50** 2689-700

Virtanen H, Keshvari J and Lappalainen R 2006 Interaction of Radio Frequency electromagnetic fields and passive metallic implants-a brief review *Bioelectromagnetics* **27** 431-9

Virtanen H, Keshvari J and Lappalainen R 2007 The effect of authentic metallic implants on the SAR distributions of the head exposed to 900, 1800 and 2450MHz dipole near field *Phys. Med. Biol.* **52** 1221-6

Wainwright P 2000 Thermal effects of radiation from cellular telephones *Phys. Med. Biol.* **45** 2363-72

Wang J, Joukou T and Fujiwara O 1998 Localized specific absorption rate in the human head in metal-framed spectacles for 1.5GHz Hand-held mobile telephones *Trans IEE of Japan* **118-A** 1234-40

Whittow W, Panagamuwa C, Edwards R and Vardaxoglou J 2007 Specific absorption rates in the human head due to circular metallic earrings at 1800MHz. In: *2007 Loughborough Antennas and Propagation Conference,* (Loughborough, UK) 277-80

Whittow W, Panagamuwa C J, Edwards R, Vardaxoglou J C and McEvoy P 2006 A study of head worn jewelry, mobile phone RF energy and the effect of differing tissue types on rates of absorption. In: *The First European Conference on Antennas and Propagation (EuCAP 2006),* (Nice, France)

Whittow W G 2004 Specific absorption rate perturbations in the eyes and head by metallic spectacles at personal radio communication frequencies. In: *PhD thesis EEE Dept.*: University of Sheffield, UK

Whittow W G and Edwards R M 2004 A study of changes to specific absorption rates in the human eye close to perfectly conducting spectacles within the radio frequency range 1.5 to 3.0GHz. *IEEE Trans. Antennas and Propagation* **52** 3207-12

Whittow W G and Edwards R M 2005 Applications of a genetic algorithm for identification of maxima in specific absorption rates in the human eye close to perfectly conducting spectacles *IEE Proceedings Science, Measurement & Technology* **152** 89-96